Ex Vivo Biomechanics of Bus Driver Whole Body Vibration Exposures in the Lumbar Spine

Lovenoor Aulck[1], Peter W. Johnson[2], Randal P. Ching[3]

Abstract This pilot study is a first attempt to translate occupational whole body vibration (WBV) exposures into a laboratory setting to better understand the biomechanical loading on the spine that may be associated with WBV-related low back pain and injury. WBV exposures experienced by bus drivers were recorded from a low-floor city bus when driving across two distinct road types – one profile was a continuous, low-amplitude exposure (representative of freeway driving) and the other an intermittent, impulsive, high-amplitude exposure (induced by raised freeway expansion joints). The exposure signals were processed to extract vibration signatures (amplitude and frequency). Then, 6 human cadaver spinal segments were exposed to one of the two exposure profiles. A novel staining technique was used to explore disc degradation resulting from the two different exposure profiles. None of the specimens exposed to the continuous, low-amplitude exposure profile demonstrated any visible damage to the intervertebral disc whereas all three of the specimens exposed to the intermittent, impulsive exposure profile demonstrated at least some signs of damage.

Keywords driving exposure, intervertebral disc, low back pain, occupational health, vertebrae

I. INTRODUCTION

Back injuries, particularly lower back pain (LBP), are amongst the most prevalent and costly non-lethal medical conditions affecting adults [1]. An association between vehicle whole body vibration (WBV) exposure and the development of LBP has been established through numerous epidemiological studies [2]. However, despite this epidemiological association, the etiological and biomechanical mechanisms of how WBV contributes to LBP and injury are not well understood. Previously, cadaveric experiments [3] and finite element analyses [4] have been used to investigate many aspects of the spine including determining resonant frequencies of vertebral structures, exploring stress-injury relationships, and outlining the effects of cyclic loading and flexion. However, studies that have used occupational WBV data to outline the displacements undergone by spinal structures in a work setting and then used these displacements to apply cyclic loads to human cadaveric spine specimens are, to the knowledge of the authors, thus far nonexistent. As such, using field-measured occupational WBV exposures translated into a controlled laboratory setting, this study exposed human lumbar spine segments to occupational vehicle WBV exposures to better understand the mechanisms of WBV-related low back injury.

The occupational exposures selected for this study were those encountered by bus drivers, who are known to have a high prevalence of LBP. The study sought to investigate the effects of two different types of WBV exposures – a highly impulsive, intermittent vibration collected as a vehicle traversed expansion joints and a less impulsive, more continuous vibration collected as the vehicle

[1]Lovenoor Aulck is a graduate of the MS in Bioengineering program at the University of Washington in Seattle, WA, USA and is currently a Whitaker Fellow at the Vrije Universiteit in Amsterdam, the Netherlands. [2]Peter W Johnson is Associate Professor of Environmental and Occupational Health Sciences at the University of Washington in Seattle, WA, USA. [3]Randal P Ching is Research Associate Professor of Mechanical Engineering at the University of Washington in Seattle, WA, USA. Correspondence: 206-625-0633, rc@uw.edu.

traversed an interstate freeway. These exposures were selected because they represent significantly different inputs to our laboratory ex vivo model with the expectation that they might provide evidence as to which of the two exposures would be more injurious to the lumbar vertebral structures.

II. METHODS

Data Collection

WBV field data were collected on low-floor city buses (13.9m long; New Flyer; Winnipeg, Manitoba, Canada) as a driver traversed a standardized route. A global positioning system (GPS) unit (Model DG-100; GlobalSat; Chino, CA, USA) was placed in the cabin of the bus to record both the speed and location of the vehicle. Just adjacent to the bus driver's seat, a floor mounted accelerometer (model 356B40; PCB Piezotronics; Depew, NY, USA) measured the z-axis (up-and-down) acceleration from the bus floor. Acceleration data was collected at 1280 Hz using an eight channel data recorder (Model DA-40; Rion Co. LTD; Tokyo, Japan) while the GPS unit logged data at 1 Hz. The standardized route consisted of two road conditions of interest for this experiment - an older freeway segment with expansion joints and a newer, smoother freeway segment. The segments were traversed at roughly the same speed averaging 91.0 and 88.7 kmph, respectively.

The floor accelerations from the bus for the two road segments were then inputted into a six-degree of freedom hydraulic shaker platform (Moog Inc.; Kirkland, WA, USA). Twelve male professional drivers were seated in an industry-standard air suspension seat (model Q91; USSC Seating; Exton, PA, USA) which was securely fixed to the top of the platform. While the floor accelerations from the bus were played into the shaker platform and identical accelerometers as the bus data collection and an eight-channel data recorder (model CoCo 80; Crystal Instruments; Santa Clara, CA, USA) were used to log the z-axis accelerations at a rate of 1280 Hz from the base of the platform, the seat top, and the chest of the subjects.

Data Processing

The servohydraulic testing system used in this experiment required vibration inputs in terms of displacements, not accelerations; as a result, the vibration acceleration profiles were converted to displacement values. Formulaically, the velocity and displacement of a body can be determined from a single and double integration, respectively, of its acceleration:

$$v(t_f) = v(t_0) + \int_{t_0}^{t_f} a(\tau)\, d\tau \qquad (Eq.1)$$

$$d(t_f) = d(t_0) + \int_{t_0}^{t_f} v(\tau)\, d\tau \qquad (Eq.2)$$

Where the variables "a," "v," and "d" symbolize acceleration, velocity, and displacement, respectively while "t" represents values in the time domain. To calculate displacement from acceleration data, three stages of dual-pass high-pass filtering (4^{th} order, 0.5 Hz cut-off) were used in conjunction with two stages of integration. The high-pass filters were used to account for accelerometer drift, DC biases, and the lack of initial conditions. A dual-pass filter was used to ensure filtering did not introduce a phase shift during any iteration of filtering. The accuracy of this method was tested and verified using accelerometers affixed to a servohydraulic piston oscillating at known displacements and frequencies.

After computing displacement values of the seat and sternum during the shaker platform data collection, 180-second segments of the two road features of interest were isolated and extracted. The expansion joints were found to impart acceleration impulses greater than 5 m/s^2 while the regions of the freeway without expansion joints generally had acceleration values less than 5 m/s^2. For the expansion joints, the mean peak-to-peak displacement was calculated for each subject and an average displacement was calculated for the 12 subjects. For the freeway segments of interest, twice the root mean square displacement was calculated (to account for upward and downward displacement) and averaged across the 12 subjects.

Mathematical Model

A mathematical model was developed to predict and verify the results extracted from the shaker table data collection. The vibration response of the seat-sternum system was mathematically modeled using a two-parameter mass-spring-damper mechanical model consisting of two components - one component modeling the vibration of the buttocks of the seated subjects and the other component to modeling the vibration of spine from the sacrum to the sternum. Both components consisted of a parallel mass-spring-damper system as shown in Fig. 1 but with differing spring and damping coefficients, as determined from literature [5, 6].

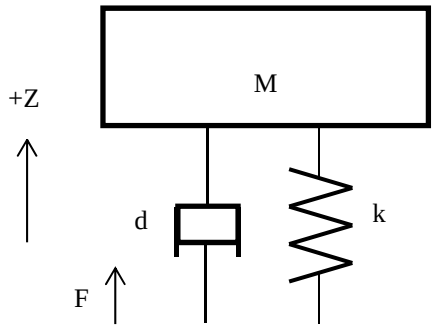

Fig. 1. Mass-spring-damper mechanical model. M, Z, F, d, and k represent the mass, vertical displacement, input force, damping coefficient, and spring coefficient of the system, respectively.

If the forces related to the mass, dashpot, and spring are Fm = Mz", Fd = dz', and Fs = kz, respectively, where single and double apostrophes indicate first and second derivatives of the position (z). Then, the sum of forces can be expressed as:

$$z'' + 2\varsigma\omega z' + \omega^2 z = \frac{F}{M} \qquad (Eq. 3)$$

with

$$\omega = \sqrt{\frac{k}{M}} \quad \text{and} \quad \varsigma = \frac{d}{2M\sqrt{kM}}$$

The differential equations associated with Eq. 3 were then used with mathematical computing software (Matlab R2009, Mathworks, Natick, MA, USA) to predict the displacement response of the buttocks and the segment of the spine between the sacrum and sternum. Displacement simulations were conducted for each of the 12 hexapod subjects for 180 seconds of seat acceleration data from both the freeway and expansion joint road segments. The displacement of the buttocks was then subtracted from the displacement values calculated from the shaker platform to estimate the displacement history of the spine. Based on the accelerometer mounted at the sternum, the resulting displacement values were then divided across seven equivalent segments below the

sternum to approximate the displacement of each intervertebral disc. The final displacement and frequency values are detailed in Table 2 and shown graphically in Fig. 3 of the Results section. The impulsive, expansion joint exposure was represented as a duty cycle consisting of two sequential impulses, one at 1.6 mm and the other at 0.8 mm. The impulses occurred 0.4 seconds apart (peak-to-peak) to correspond to the 2.5 Hz frequency of the vibrations; the duty cycle was imparted every 2 seconds to correspond to the 0.5 Hz rate at which the expansion joints are encountered by drivers (expansion joints spaced approx. 50 m apart and vehicle travelling approx. 90 kmph). The continuous, freeway exposure, meanwhile, was represented as a continuous waveform cycling at 2.5 Hz with a peak-to-peak amplitude of 0.34 mm.

Cadaveric Experiments

Six human cadaveric lumbar functional spinal units (FSUs) with intervertebral discs able to maintain intradiscal pressure at 90 PSI were prepared. The six specimens are detailed in Table 1 – specimens with the same number indicate segments taken from the same donor. The posterior structures of the vertebral bodies were removed along with all musculature and ligamentous tissue resulting in body-disc-body segments for testing. The ends of each test specimen were then potted in a polymethylmeth-acrylate (PMMA) mold.

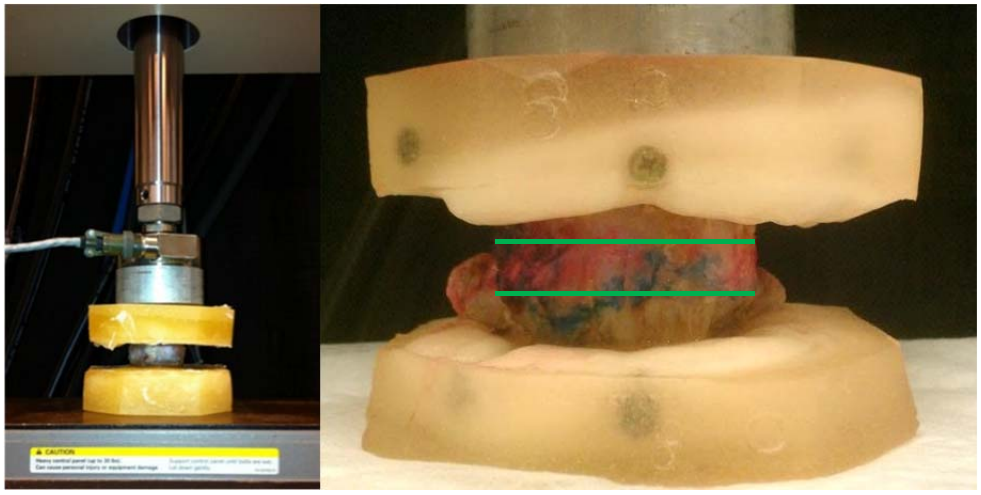

Fig. 2. (Left) Image of loading setup showing a specimen potted in PMMA with the piston of the servohydraulic testing system resting above it. Note how the setup is designed to provide uniaxial loading to the specimen. (Right) Closeup of a different potted specimen. Green lines indicate approximate location of the intervertebral disc. Specimen is colored pink and blue on the exterior as a result of overflow from the staining technique used.

The potted specimens were mounted in a servohydraulic testing system (model 810; MTS; Eden Prairie, MN, USA) and continuously exposed to one of the two vibration signatures. The loading signatures were applied along a single axis (along the cranial-caudal axis of the vertebral bodies), thereby minimizing any lateral loading, movement, or bending of the specimens. The experimental setup is shown in Fig. 2. The specimens were cycled for 2.4 hours of driving exposure to one of the two vibration signatures (21,600 cycles for continuous, freeway exposure and 4320 cycles for impulsive, expansion joint exposure). Both correspond to a driving distance of approximately 215 km. A bi-colored staining technique consisting of safranin-O and alcian blue stains was used to visually differentiate preexisting damage to the intervertebral disc from damage induced by the cycling protocol. The safranin-O stain was injected into the nucleus pulposus prior to cycling, thereby giving a red outline to highlight any preexisting damage to the annulus fibrosis of the disc; the alcian blue was injected at the beginning, one-third, two-thirds, and at the end of cycling to give an indication of the location of the nucleus pulposus before, during, and after testing. The staining

technique used was simply to elucidate gross damage to the disc/endplates imparted by the cyclic loading protocols. Histological analyses were not a part of the experimental protocol. All injections were made with maximal thumb pressure or up to 1 ml. After cycling, the intervertebral discs were dissected to determine whether there was any structural deterioration and/or disc damage.

TABLE 1
OVERVIEW OF SPECIMENS USED IN TESTING

Specimen #	*Age at death*	*Segment*	*Exposure*
1	65 years	L4-L5	Exp. Joint
2	61 years	L2-L3	Freeway
3a	21 years	L2-L3	Exp. Joint
3b	21 years	L4-L5	Freeway
4a	54 years	L2-L3	Freeway
4b	54 years	L4-L5	Exp. Joint

III. RESULTS

TABLE 2
RESULTS FROM DISPLACEMENT SIGNATURE CALCULATIONS

Segment	*Amplitude*	*Frequency*
Freeway	0.34 mm	2.5 Hz
Expansion Joints	1.6 mm & 0.8 mm	2.5 Hz & 0.5 Hz

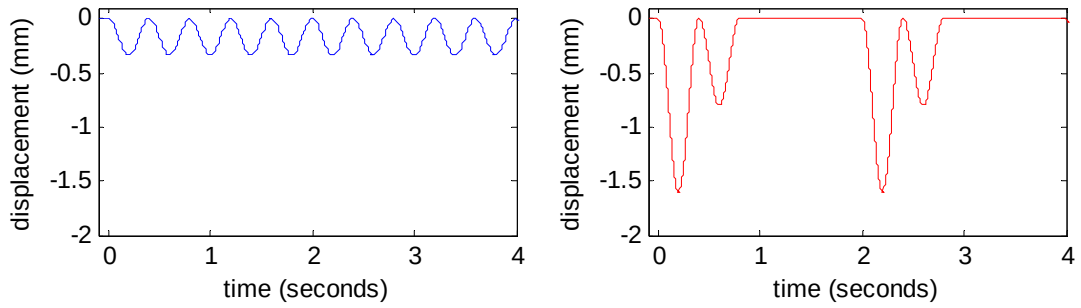

Fig. 3. Cycling waveforms for the freeway (blue) and expansion joint (red) vibration signatures. Negative displacement values reflect the downward movement of the MTS piston on the potted test specimen.

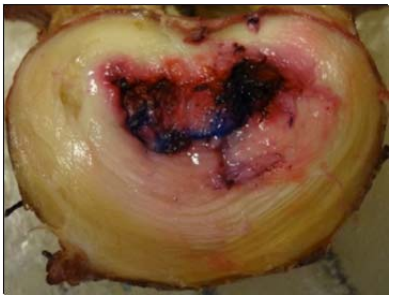

Fig. 4. Disc exposed to continuous, low-amplitude freeway signature. Note how the blue/purple nucleus pulposus remained within the outline of the safranin-O dye, thereby

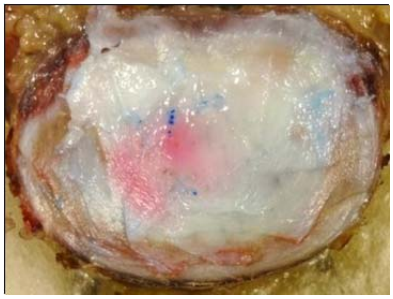

Fig. 5. Endplate of specimen exposed to the freeway signature. Note the lack of an endplate fracture. Specimen 3b, L4-L5.

indicating a lack of damage to the annulus fibrosus. Specimen 4a, L2-L3.

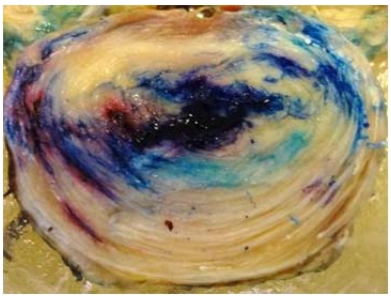

Fig. 6. Disc exposed to intermittent, impulsive freeway signature. Note how the blue/purple stain extended beyond the outline of the safranin-O dye, thereby indicating damage to the annulus fibrosus. Specimen 4b, L4-L5.

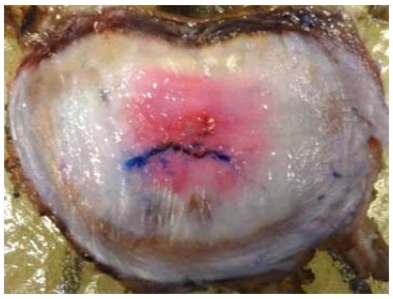

Fig. 7. Endplate of specimen exposed to the expansion joint signature. Note the prominent blue endplate fracture. Specimen 3a, L2-L3.

TABLE 3
RESULTS FROM SPECIMEN TESTING

Specimen #	*Segment*	*Exposure*	*Annulus Damage*	*Endplate Fracture*
2	L2-L3	Freeway	-	-
3b	L4-L5	Freeway	-	-
4a	L2-L3	Freeway	-	-
1	L4-L5	Exp. Joint	✓	✓
3a	L2-L3	Exp. Joint	-	✓
4b	L4-L5	Exp. Joint	✓	✓

IV. DISCUSSION

During cycling, none of the specimens exposed to the continuous, low-amplitude smooth freeway cycling protocol demonstrated any visible damage to the intervertebral disc. The intervertebral discs were able to maintain intradiscal pressure throughout the testing procedure (injections were made using thumb pressure applied against maximal resistance). Additionally, the nucleus pulposus remained within the area outlined by the safranin-O stain and no visible deterioration of the annulus fibers was detected upon dissection of the discs. The specimens did not have an endplate fracture on either the superior or inferior endplates adjacent to the intervertebral disc upon dissection.

All three of the specimens exposed to the impulsive, intermittent rough freeway cycling protocol demonstrated at least some signs of damage induced by cycling. Endplate fractures were found on the inferior of the two endplates adjacent to the intervertebral disc for all three specimens. All three specimens were unable to maintain intradiscal pressure during injections. Two of the three intervertebral discs also showed signs of deterioration of the inner annulus and migration of either/both alcian blue stain and nuclear material beyond the inner annulus. The disc that did not demonstrate any damage to the annulus fibrosis was from a relatively young donor and was therefore of very good health. The results for all 6 of the specimens used during final testing are

summarized in Table 3. It should be noted that these results are preliminary and more samples are needed to provide a statistical basis for comparison.

The change and damage to the intervertebral discs and end plates under the relatively short duration of impulsive loading seemed rather exceptional. Some possible explanations for this rapid deterioration could include the ages of the specimens tested, the fact that there were no facet joints, the lack of rest between impulsive exposures, or some combination of these factors.

V. LIMITATIONS

One limitation of this study was the use of body-disc-body test specimens. While serving to better control the exposures to the intervertebral disc (especially in the case of facet arthrosis), removal of the posterior structures may have altered the natural displacement of the discs. Planned future studies will investigate this effect. Additionally, future FSU testing will keep facet joints intact which may result in less damage and more realistic time estimates for tissue deterioration and/or damage. Additionally, the loading limit of the spine is also substantially affected by the amount of intact musculature. Leaving muscular structures intact would provide a greater association between experimental results and clinical observations; however, for this particular experiment, a body-disc-body model was utilized to provide the simplest model to explore our hypothesis.

Another limitation of this study was that the FSUs were predominantly from older subjects which may have accelerated the degree to which deterioration occurred during the tests. However, obtaining FSUs from younger cadaveric specimens, which may be more representative of the general population, remains a challenge due to a lack of supply. The relatively small number of specimens used also relates to the availability of intact spine specimens. Additionally, the desire for paired specimens further limited the availability of suitable test specimens. Future tests will are planned in which the number of specimens tested is increased to a level where statistical and physiological significance can be determined.

A third limitation of the study was the manner in which displacements of individual intervertebral segments were derived. The procedure relied on using a hydraulic shaker platform to reproduce field-collected acceleration data. Current field data collection protocols now include sternum accelerometry which will obviate the need for shaker platform testing.

VI. CONCLUSIONS

Based on the presented results, evidence exists that for an equal driving-time exposure, higher impulses from features of freeways such as expansion joints are more likely to induce damage to the intervertebral discs and or end plates than the vibration induced from driving on a more even (smooth) driving surface. These injuries can be manifested as either endplate fractures and/or deterioration of the annulus of the intervertebral disc, which can lead to disc prolapse and/or herniation. However, based on the small sample number (n = 6), further research is required to more systematically analyze these types of occupationally-induce WBV exposures. Nevertheless, this preliminary study was an important first step in developing an experimental model to explore the effects of real-world occupational WBV exposures on the lumbar spine.

VII. ACKNOWLEDGEMENT

The authors would like to thank Ryan Blood for his work with the bus and shaker platform vibration data collection.

VIII. REFERENCES

[1] Deyo RA, Tsuiwu YJ, Descriptive epidemiology of low-back-pain and its related medical-care in the United States, *Spine*. 12, 264-268, 1987.

[2] Bovenzi M, Hulshof CTJ, An updated review of epidemiologic studies on the relationship between exposure to whole-body vibration and low back pain (1986-1997), *International Archives of Occupational and Environmental Health*. 72, 351-365, 1999.

[3] Potvin JR, Occupational spine biomechanics: A journey to the spinal frontier, *Journal of Electromyography and Kinesiology.* 18, 891-899, 2008

[4] Natarajan RN, Williams JR, Andersson GBJ, Recent advances in analytical modeling of lumbar disc degeneration, *Spine*, 29, 2733-2741, 2004

[5] Keller TS, Colloca CJ, A rigid body model of the dynamic posteroanterior motion response of the human lumbar spine. *Journal of Manipulative and Physiological Therapeutics*. 25, 485-496, 2002

[6] Aimedieu P, Mitton D, Faure JP, et al. Dynamic stiffness and damping of porcine muscle specimens. *Medical Engineering & Physics.* 25, 795-799, 2003